

RETRIEVING LST AND ITS THERMAL ENVIRONMENT EVALUATION ANALYSIS BASED ON CBERS-02 IRMSS AND MODIS DATA

YU Ming^{a,b,*}, JI Qing^b, SHU Qiong^a

(^a East China Normal University Key Lab of Geographic Information Science, Ministry of Education, 200062, China)

(^b School of Geographical Sciences, Fujian Normal University, Fuzhou 350007, China)

yumingfz@vip.sina.com

KEY WORDS: CBERS-02 IRMSS; Land Surface Temperature (LST); Atmospheric Water Vapour Content; Human Body Comfort Index; Thermal Environment Evaluation

ABSTRACT:

The thermal environment and thermal effect is one of the most important contents in city climate and environment researches. Retrieving and analyzing land surface temperature (LST) is an efficient way to research thermal environmental problem of earth surface. Taking Fuzhou as the study area, this paper uses CBERS-02 IRMSS thermal infrared remote sensing data for generalized single-channel algorithm developed by Jiménez-Munoz and Sobrino to inverse surface temperature. MODIS data received on the same day was used to compute the atmospheric water vapour content in the pixel scale which is a important parameter for the algorithm. Based on the results of the inversion, we introduce the human body comfort index to evaluate the urban thermal environment of Fuzhou by revising its evaluation system. The results show that the combinations of multi-satellite remote sensing data can the accuracy of the surface temperature inversion. And the HCI method can be effectively used to describe the quality of urban thermal environment.

1. INTRODUCTION

It is an undeniable fact that in recent years, global climatic change, which becomes increasingly serious, has aroused the shared concern of countries around the world. Land surface temperature (LST) is important physical parameters of the interaction between the earth and atmosphere system which reflects the results of their energy and material exchange, and also is a key factor of surface physical processes at regional and global scales. So LST was deeply studied and widely applied in vegetation ecology, crops yield and drought monitoring, and so on. Urban thermal environment is the comprehensive performance of urban spatial environment which has a profound impact on urban climate, ecological environment and living environment with different patterns of thermal environment. In recent years, with the development of remote sensing technology and human concerns of the urban environment, urban thermal environment was caught more and more attention. Many scholars home and abroad achieved a series of achievements^[1-6] though inverting LST based on TM/ETM data so as to study urban heat island effect and thermal environment. Therefore, how to make use of remote sensing data to obtain precise urban surface temperature is an important element quantitative study of remote sensing, but also is of great significance on the study field of urban thermal environment.

In this paper, Fuzhou was selected as a study area to simulate the surface temperature and the evolution of thermal environment based on the CBERS-02 IRMSS and MODIS data.

2. STUDY AREA AND DATA

Fuzhou is the capital of Fujian province, located in the southeast Fujian province and the western side of Taiwan strait, lies between 118 ° 08 ' ~ 120 ° 31'E, and 25 ° 15 ' ~ 26 ° 39'N(seeing figure 1). The study area climate is warm and humid of typical subtropical monsoon, with annual average temperature of 17 °C ~ 22 °C and the average rainfall of 1400mm ~ 2000mm. Fuzhou is the basin topography on the whole, terrain inland from the northwest to the southeast coast tilt, the urban area of Fuzhou is located in the heart of the basin with the eastern and northern hills to the mountains, the southern plains. Minjiang River flows from northwest to southeast. As Fuzhou has north-easterly prevail winds in summer, the openings to the sea is very small, relatively closed terrain, combined with the topography and the building block which is not conducive to air flow, resulting in a higher urban temperatures especially in summer afternoon with the temperatures up to above 36 °C. Recently, with the speeding-up urbanization, The thermal environment of Fuzhou had declined with the expansion of city magnitude and buildings, the decrease of green area.

In this paper, the data acquired to inverse the atmospheric water vapour content and LST in Fuzhou were MODIS and CBERS-02 IRMSS data respectively with the same collecting phase of November 20th, 2004, as well as meteorological data, urban land use maps and other relevant data.

* Corresponding author. yumingfz@vip.sina.com

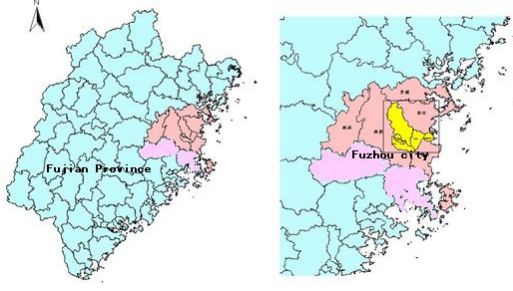


Figure 1 location map of study area

3. METHOD AND DISCUSS

3.1 Selecting Algorithm

Analyzed the characteristics of CBERS-02 IRMSS data and the actual situation of the study area, universal single-channel algorithm^[7] was adopted to retrieve LST. This algorithm does not require too much real-time data and be applicable to different satellite sensors. In this paper, the inversion process could be expressed by formula (1)(including ①~⑥):

$$T_s = \gamma \left[(\psi_1^{IRMSS9} L_{sensor} + \psi_2^{IRMSS9}) / \varepsilon + \psi_3^{IRMSS9} \right] + \delta \quad ①$$

where, T_s represents the surface temperature (K); L_{sensor} is the radiance of IRMSS sensor ($W \cdot m^{-2} \cdot sr^{-1} \cdot \mu m^{-1}$), ε is the surface emissivity; γ , δ are variables and ψ_1^{IRMSS9} , ψ_2^{IRMSS9} , ψ_3^{IRMSS9} are the function of atmospheric^[8], could be calculated by the following formula respectively:

$$\gamma = \left[\frac{C_2 L_{sensor}}{T_{sensor}^2} \left(\frac{\lambda^4}{C_1} L_{sensor} + \frac{1}{\lambda} \right) \right]^{-1} \quad ②$$

$$\delta = T_{sensor} - \gamma \times L_{sensor} \quad ③$$

$$\psi_1^{IRMSS9} = 0.01642w^3 - 0.00662w^2 + 0.13314w + 0.99253 \quad ④$$

$$\psi_2^{IRMSS9} = -0.10563w^3 - 0.33896w^2 - 1.91005w + 0.23545 \quad ⑤$$

$$\psi_3^{IRMSS9} = -0.05495w^3 + 0.39116w^2 + 0.98775w - 0.08896 \quad ⑥$$

Equation ②,

$$C_1 = 1.19104 \times 10^8 W \cdot \mu m^4 \cdot m^{-2} \cdot sr^{-1},$$

$$C_2 = 1.43877 \times 10^4 \mu m \cdot K;$$

Where, T_{sensor} is brightness temperature (K); λ is effective wavelength (for IRMSS9, $\lambda = 11.245$ ^[9]); w is the total atmospheric water content (g/cm^2).

3.2 Inversion Parameters and Discussion

So as to extract LST and evaluate the thermal environmental, some important parameters required to be determined. This paper summed up in four steps.

Step 1: Convert the gray value data (DN value) in IRMSS data into the corresponding radiance values (L_{sensor}) though formula (2).

$$L_{sensor} = \frac{DN - 44.92}{8.53} \quad (2)$$

Step 2: According to the radiation temperature (L_{sensor}), calculated brightness temperature (T_{sensor}) by the back stepping Planck equation which shown in formula (3).

$$T_{sensor} = \frac{hc}{\lambda k} \left[\ln \left(\frac{2\pi hc^2}{\lambda^5 L_{sensor}} + 1 \right) \right]^{-1} \quad (3)$$

where, h is the Planck constant, $h = 6.63 \times 10^{-34} J \cdot s$; c is the light speed at vacuum, $c = 3 \times 10^8$; λ is the effective wavelength,

$\lambda = 11.245$; k is the Boltzmann constant, $k = 1.38 \times 10^{-23}$.

Step 3: Estimation of surface emissivity. After summing up the results of previous studies^[11-13], we conducted supervised classification which was divided into three kinds of types of water, natural surfaces and built-up. Valour model was then utilized to estimate surface emissivity. As to MODIS data, corresponding to CH1 (red channel) and CH2 (near infrared channel) were calculated normalized difference vegetation index (NDVI) and the vegetation coverage (P_v),

(1) For a water pixel: ε can be replaced by a typical water emissivity, this paper calculated the corresponding thermal IRMSS infrared radiation, eventually taking $\varepsilon_{water} = 0.995$;

(2) For natural surface pixel: Natural surface is the surface comprises a mix of vegetation and bare soil cover types ($NDVI_s \leq NDVI \leq NDVI_v$), pixel emissivity could be calculated by equation (4):

$$\varepsilon_{surface} = P_v \cdot r_v \cdot \varepsilon_v + (1 - P_v) \cdot r_s \cdot \varepsilon_s + d\varepsilon \quad (4)$$

where, NDVI represents Normalized Difference Vegetation Index, $NDVI_v$ and $NDVI_s$ were the NDVI value completely bare soil and vegetation respectively; P_v is vegetation coverage, ε_v is the radiation rate of vegetation, in this paper, $\varepsilon_v = 0.985$ ^[14] while ε_s is the radiation rate of bare soil, $\varepsilon_s = 0.973$ taking ASTER laboratory spectra of soil emissivity on average to replace the bare soil emissivity value; r_v and r_s are the temperature ratio of vegetation and bare soil respectively, computed by equation (5) and (6):

$$r_v = 0.9332 + 0.0585P_v \quad (5)$$

$$r_s = 0.9902 + 0.1068P_v \quad (6)$$

$d\varepsilon$ stands for geometric distribution of surface and internal scattering effect, approximation expressed by formula(7)

$$d\varepsilon = (1 - \varepsilon_s)(1 - F)\varepsilon_v \quad (7)$$

where, F is the terrain factor, select the average value 0.55 according to different geometric distribution^[12].

(3) For built-up pixel: which is surface cover of the building surface and green vegetation ($NDVI \geq NDVI_m$), pixel emissivity could be calculated according to formula (8):

$$\varepsilon_{built-up} = P_v \cdot r_v \cdot \varepsilon_v + (1 - P_v) \cdot r_m \cdot \varepsilon_m + d\varepsilon \quad (8)$$

where, $NDVI_m$ is the NDVI value of complete building surface; ε_m is the emissivity of the building surface, $\varepsilon_m = 0.968$, according to the average field measured data from MODIS UCSB Emissivity Laboratory (URL: <http://www.icess.ucsb.edu/modis/EMIS/html/em.htm1>); $d\varepsilon$ would be calculated similar to the above; r_m is the temperature ratio of the building surface, calculated though formula(9).

$$r_m = 0.9886 + 0.1287P_v \quad (9)$$

Where, P_v represents vegetation coverage appeared in the above formulas could be calculated by formula (10) [15]:

$$P_v = \left(\frac{NDVI - NDVI_s}{NDVI_v - NDVI_s} \right)^2 \quad (10)$$

And, when $NDVI > NDVI_v$, P_v equal to 1; when $NDVI < NDVI_s$, P_v equal to 0; $\varepsilon = \varepsilon_s = 0.975$; When $NDVI > NDVI_m$, $\varepsilon = \varepsilon_m = 0.968$. Meanwhile $NDVI$ calculated from MODIS data should be resampled to 156m, to match the IRMSS band 9.

Step 4: The inversion of Atmospheric water content. Usually, Atmospheric water content was simulated through standard atmospheric by atmospheric model software, such as experience formula or MODTRAN, but the real-time atmospheric profile data were very limited, therefore, the results of this simulation accuracy can hardly be guaranteed, and the results were obtained only point data, those can not reflect the spatial distribution and differences. The channel ratio method of MODIS data to inverse atmospheric water content has a good result which has been used by some people. In this paper, we used this method to experiment at pixel scale of atmospheric water vapour content, using (11) to compute [17, 18]:

$$w = 0.192w_{17} + 0.453w_{18} + 0.355w_{19} \quad (11)$$

where, W_{17} , W_{18} , W_{19} are the water vapour content of channels 17,18 and 19 of MODIS water absorption channels respectively.

$$w_{17} = 26.314 - 54.434(L_{17}/L_2) + 28.449(L_{17}/L_2)^2 \quad (12)$$

$$w_{17} = 5.012 - 23.017(L_{18}/L_2) + 27.884(L_{18}/L_2)^2 \quad (13)$$

$$w_{17} = 9.446 - 26.887(L_{19}/L_2) + 19.914(L_{19}/L_2)^2 \quad (14)$$

where, L_{17} , L_{18} , L_{19} and L_2 are radiation intensity which are received by channe17,18,19 and 21, and radiation intensity (L) can be computed by (15).

$$L = radiance_scales(SI - rasiance_offsets) \quad (15)$$

where, radiance scales and rasiance offsets are the radiance pantograph ratio and radiation intercept of different band, SI is the storage value of MODIS 1B data.

4. RESULT AND ANALYSIS

4.1 Atmospheric moisture content distribution

To calculate the atmospheric moisture content of study area with the formula (11) and resample to the spatial resolution of

156m, which matched the CBERS-02 IRMSS thermal infrared data, the final results were shown in figure 2.

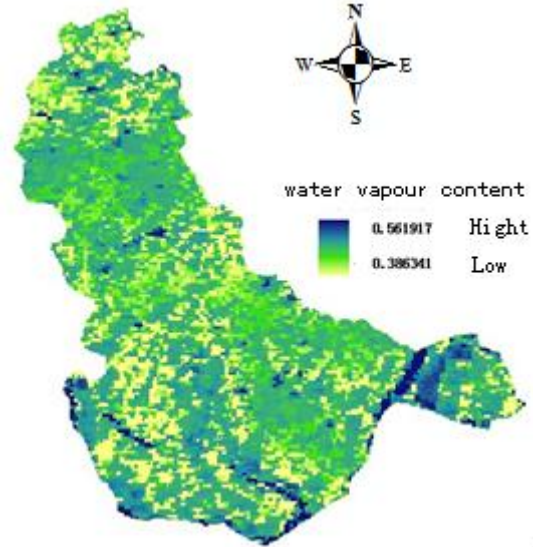


Figure2 Distribution of atmosphere water vapour content of Fuzhou on Nov.20th, 2004

As was demonstrated in figure 2, the range of atmosphere water content was from 0.386 to 0.562g/cm² in Fuzhou while the area of Minjiang River were mostly more than 0.5g/cm² which was higher than other regions significantly, but atmosphere water content of urban was about 0.42 g/cm², this was because of the larger evaporation of the surface. It reflected that the different land cover types result in the larger difference of spatial distribution of the atmospheric water content. Therefore, if used the value of atmospheric water content of individual ground-based observations to replace the entire regions, there will be large errors to carry out the inversion of surface temperature. This paper will use the parameters of the atmospheric water content of MODIS at pixel scale to inverse the surface temperature, which can improve the accuracy of inversion.

4.2. Surface temperature inversion results map

With the formula of surface temperature inversion, the surface temperature spatial distribution of Fuzhou was shown in Figure 3.

As demonstrated in Figure 3, the surface temperature of urban areas was relatively high, higher than the surrounding suburb areas significantly, the boundaries of high temperature zone was discernible clearly, was more uniform with the urban contour. The temperature of the area with good vegetation cover and water were corresponding low temperature zone, which showed a clear negative correlation between temperature and Normalized Difference Vegetation Index (NDVI). Because of the rivers, there were obvious linear low-temperature zone which extended with the shape of river in some places. High temperature concentrated in the area of urban, with the concentration of human activities and densely distribution of buildings. At the internal of Urban Heat Island, the differences of surface temperature was also very significant, the regions had a corresponding lower surface temperature, with good green vegetation and water. For example, the Gaogai mountain of Cangshan District had the obvious low temperature because of the good vegetation cover.

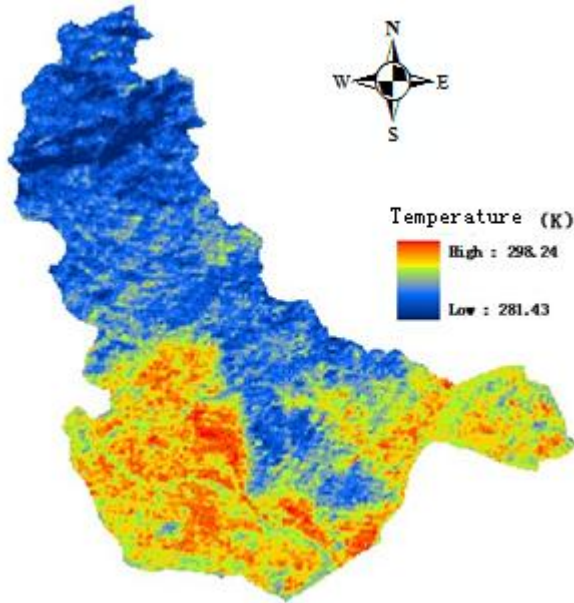


Figure3 Retrieved LST of Fuzhou on Nov.20th, 2004

The typical high-temperature regions were: Taijiang District, Xindian and Fuxing investment Zone of Jinan District, and the axis region includes Cangqian, Xiadu, Shancha street of Cangshan District, Gaishan investment Zone and Chenmen investment zone. The Mawei district and Langqi economic development zones also had higher temperature. Most of these high temperatures regions were residential living quarters, busy commercial districts and industrial zones, with density population, much man-made heat, many dense buildings and relative low vegetation coverage, resulting in a strong distribution of high temperature.

4.3 Urban thermal environmental evaluation of Fuzhou

Urban thermal environment as an important aspect of the ecological environment have an existence of space-time interaction and interdependence relation between urban climate, urban ecology and urban disasters, urban thermal environment has a deep effects on city micro-climate, air quality, energy consumption structure, and public health and so on [19]. At a certain spatial and temporal scale, the change of urban surface temperature, reflect the energy balance relationship in biology, physics, chemistry of the city, and form a different city hot field distribution characteristics. As a status indicator of surface energy, temperature profoundly depicts the composition of substances urban thermal properties and geometric structures of the environment co-decide thermal features, and this is a variety of energy flow process general expression. This paper attempts to introduce human comfort index and modify the corresponding evaluation system based on inversion of surface temperature and atmospheric water content, and at last evaluate and analyze thermal environment of Fuzhou quality.

Some scholars had raised climate physiological indicators [], with the progress of further study, the physiological indicators of climate were constantly improved and perfected. At present, The commonly used physiological indicators of climate was human comfort index (K), which formula (16) was calculated as follows[20]:

$$K = 1.8t - 0.55(1.8t - 26)(1 - f) - 3.25\sqrt{v} + 32 \quad (16)$$

where, K stands for human comfort index; t stands for temperature ($^{\circ}\text{C}$); v stands for the speed of wind (m / s); f stands for the relative humidity, which can be expressed as formula (17) in meteorology:

$$f = \frac{e}{E} \times 100\% \quad (17)$$

where: e stands for surface pressure (hPa), which can be calculated by the anti-solution of atmospheric water content in accordance with the experiment expression (18) and (19) [21] put forward by Yang Mei-jing.

$$w' = a_0 + a_1e + a_2e^2 \quad (18)$$

$$w = c_0 + c_1w' \quad (19)$$

Where, w' stands for atmospheric precipitation, w stands for atmospheric water vapour content, a_0 , a_1 , a_2 , c_0 , c_1 are experience factor, as for Fuzhou, $a_0 = -0.2232$, $a_1 = 0.2788$, $a_2 = -0.0027$, $c_0 = 0.0956$, $c_1 = 0.7412$;

E stands for ground water saturation pressure (hPa), which calculated in accordance with Magnus empirical formula (20) [22] generally :

$$E = 6.11 \times 10^{\frac{7.5t}{273.15+t}} \quad (20)$$

However, the inversion temperature from remote sensing image is land surface temperature which is difference in human comfort index model. So, this study directly made use of surface temperature instead of air temperature to calculate human comfort index on the basis of amendment the evaluation system, expressed in the formula (21).

$$HCI = 1.8(T_s - 273.15) - 0.55[1.8(T_s - 273.15) - 26] \quad (21)$$

$$\left(1 - e / 6.11 \times 10^{\frac{7.5(T_s - 273.15)}{T_s}}\right) - 3.2\sqrt{v} + 32$$

where, HCI stands for human comfort index based on LST geothermal-; T_s is land surface temperature; e is surface pressure and v is the speed of wind.

After inversed atmosphere water content and LST based on MODIS data and CBERS-02 IRMSS thermal infrared data, as well as the wind speed data from Meteorological Science Research Institute of Fujian Province and the actual situation of the study area, we generated human comfort index classification map of Fuzhou (Figure 3) according to the evaluation system proposed by Zhang Shuyu (Table 1) and classification standards of China Meteorological Administration.

Table 1 Grades of human body comfort index and human sensation

Class	Index range	Feeling
e	$HCI < 31$	Very cold, uncomfortableness
d	$31 \leq HCI < 44$	Cold, uncomfortableness
c	$44 \leq HCI < 56$	cold more, uncomfortableness
b	$56 \leq HCI < 68$	Cool, comfort

A	$68 \leq \text{HCI} < 72$	Very comfort
B	$72 \leq \text{HCI} < 79$	More warm, comfort
C	$79 \leq \text{HCI} < 83$	hot, more uncomfortableness
D	$83 \leq \text{HCI} < 88$	Hot, uncomfortableness
E	$\text{HCI} \geq 88$	Very hot, uncomfortableness

It can be seen from Figure 4, Fuzhou performances the cool and cold thermal environment characteristics overall at November 20th, 2004, while the main district of the city performance comfort and warm. The regions which people feel cold mainly located at Rixi town with higher altitude and good vegetation, and the regions people feel less hot were rare, scattered in urban areas. The evaluation results of HCI were in good tune with the measure data of weather station, which reflected the human comfort index of evaluation method with the inversion parameters based on remote sensing could be effective used to describe urban spatial characteristics of thermal environment.

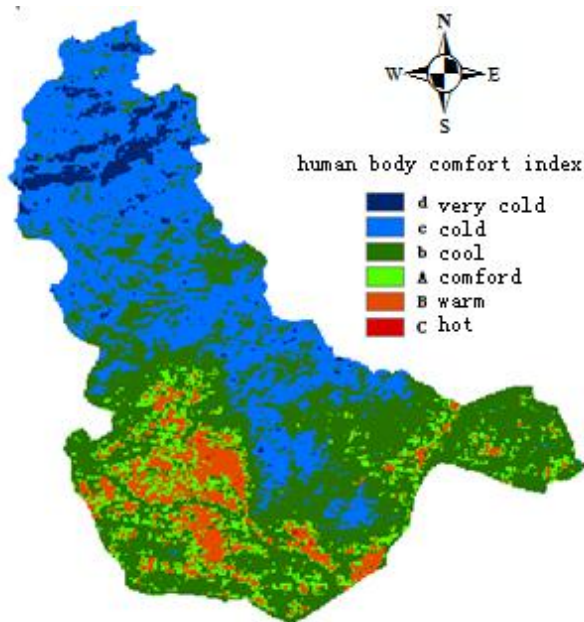


Fig.4 Classification map of human body comfort index in Fuzhou on Nov.20th, 2004

5. CONCLUSION

In this paper, Fuzhou was selected as a study area to inverse surface temperature adopted single-channel algorithm based on CBERS-02 IRMSS thermal infrared data using atmosphere water content which derived from MODIS data of the same phase. Results show that, CBERS-02 IRMSS thermal infrared remote sensing data have good surface temperature inversion capability and enormous potential with important application value of urban thermal environment effect and its spatial distribution studies.

MODIS data combined with CBERS-02 IRMSS data could bring into full play to the advantages of multi-source data, improved the accuracy of inversion atmospheric water vapour content, and obtained more reasonable results of the surface temperature.

Human comfort index evaluation model was a simple and effective method to evaluate urban thermal environment based on inversion results of surface temperature and atmospheric water content, to describe urban thermal environment spatial characteristics. In future research, we will do further study to make this method to be universal application.

ACKNOWLEDGEMENTS

This work was funded by LGISEM0810 and 2006Y0008 Programs. We thank the institute of meteorological science of Fujian province for providing us MODIS data.

REFERENCES

- [1] Gu D, Gillespie A. A new Approach for Temperature and Emissivity Separation[J]. *International Journal of Remote Sensing*, 2000, 21:2127~2132.
- [2] ZHOU Hong-mei, ZHOU Cheng-hu, et al. The Surveying on Thermal Distribution in Urban Based on GIS and Remote Sensing[J]. *Acta geographica sinica*, 2001, 56(2):189~196.
- [3] Weng Q H. Fractal Analysis of Satellite-detected Urban Heat Island Effect[J]. *Photogrammetric Engineering and Remote Sensing*, 2003, 69(5): 555~566.
- [4] J.A.Voogt, T.R.Oke. Thermal remote sensing of urban climates[J]. *Remote Sensing of Environment*, 2003, 86(3):370~384.
- [5] GONG A-du, JIANG Zhang-yan, LI Jing, CHEN Yun-hao, HU Hua-lang. Urban Land Surface Temperature Retrieval Based on Landsat TM Remote Sensing Images in Beijing [J]. *Remote Sensing Information*, 2005(3):18~20.
- [6] YANG Ying-bao, SU Wei-zhong, JIANG Nan. Time-Space Character Analysis of Urban Heat Island Effect in Nanjing City Using Remote Sensing[J]. *Remote Sensing technology and application*, 2006, 21(6):488~192.
- [7] Jiménez-Munoz J C, Sobrino J A. A Generalized Single-Channel Method for Retrieving Land Surface Temperature from Remote Sensing Data[J]. *Journal of Geophysical Research*, 2003, 108(D22):4688~4695.
- [8] ZHANG Yong, YU Tao et al. Land Surface Temperature Retrieval from CBERS-02 IRMSS Thermal Infrared Data and Its Applications in Quantitative Analysis of Urban Heat Island Effect[J]. *Journal of Remote Sensing*, 2006, 10(5):789~797.
- [9] LIU San-chao, LIU Qin-huo, GAO Mao-fang, LIU Qiang. A Study on Effects of Spectral Response Function and Band Width on Land Surface Temperature Inversion[J]. *Remote Sensing Information*, 2007(5):3~6.
- [10] ZHANG Yong, YU Tao, et al. Radiometric calibration of CBERS-02 IRMSS Thermal Infrared Band[J]. *Science in china (series E)*, 2005, 35(supplementary issue I):70~88.

- [11] Li Zhao-liang, Petitcolin F, Zhang R H. A physical algorithm of inversion the surface emissivity from middle infrared and thermal infrared data[J]. *Science in china (series E)*, 2000,30 (supplementary issue) :18~26.
- [12] Enric Valor,Vicente Caselles.Mapping land surface emissivity from NDVI:Application to European.African and south American areas[J]. *Remote Sensing of Environment*, 1996(57):167~184.
- [13] Snyder W C, Wan Z, Zhang Y,et al.Classification-based Emissivity for Land Surface Temperature Measurement from Space [J]. *International Journal of Remote Sensing*, 1998, 19(14): 2753~2774.
- [14] Sobrino J A,Caselles V,Becher F.Signification of the Remotely Sensed Thermal Infrared Measurements Obtained Over a Citrus Orchard[J]. *ISPRS Photogrammetric Engineering and Remote Sensing*,1990,44:343~354.
- [15] Carlson T N, Ripley D A.On the relation between NDVI,fractional vegetation cover, and leaf area index[J]. *Remote Sensing of Environment*, 1997,62 (3):241~252.
- [16] Meng Xian-hong, Lu Shi-hua, Zhang Yu etal . The study on airspace atmospheric water vapor based on modis data in Jinta oasis [J]. *Progress of Water Science*, 2007,18(2):264~269.
- [17] Sobrino J A, Kharraz J EL.Surface temperature and water vapor retrieval from MODIS data [J]. *International Journal of Remote Sensing*, 2003, 24(24):5161~5182.
- [18] JIANG Li-peng1, QIN Zhi-hao, Xie Wen. Retrieving atmospheric water vapour from modis near infrared data[J]. *Remote Sensing for Land & Resources*, 2006(3):5~9.
- [19] The Remote Sensing analysis of urban Heat Environment : structure , process , simulate and influence[M].Beijing: science press, 2004.
- [20] XU Dong-bei1, WANG Xiao-yong, HUANG Yu-xia etc. The Study on Forecasting System for Comfort Index of Human Body in LanZhou[J]. *Gansu Meteorology*, 2003, (3):20~23.
- [21] Yang Jing-mei,Qiu Jin-huan. A method for Estimating Precipitable Water and Effective Water VaPor Content from Ground Humidity Parameters [J]. *Chinese Journal of AtmosPheric Science*, 2002, 26(1): 9~22.
- [22] Zhou Shu-zhen. Meteorology and Climatology (the third edition) [M].Beijing: Higher Education Press,1997.
- [23] Zhang Shu-yu. The Weather Forecast Techniques of Urban Environment [M]. Beijing: Meteorology Press, 2002.